Functional Reconstitution of the Large-Conductance, Calcium-Activated Potassium Channel Purified from Bovine Aortic Smooth Muscle†

Kathleen M. Giangiacomo,*,‡ Margarita Garcia-Calvo,§ Hans-Gunther Knaus,§ Theodore J. Mullmann,‡ Maria L. Garcia,§ and Owen McManus§

Biochemistry Department, Temple University School of Medicine, 3420 North Broad Street, Philadelphia, Pennsylvania 19140, and Department of Membrane Biochemistry and Biophysics, Merck Research Laboratories, P.O. Box 2000, Rahway, New Jersey 07065

Received July 26, 1995; Revised Manuscript Received September 25, 1995⊗

ABSTRACT: The charybdotoxin (ChTX) receptor has been purified from bovine aortic smooth muscle using conventional chromatographic techniques and sucrose gradient centrifugation. Fractions from the final sucrose gradient purification were enriched in specific binding of monoiodinated ChTX (^{125}I-ChTX) approximately 2000-fold over native sarcolemmal membranes. The ChTX binding activity correlated with the presence of two polypeptides of 65 (α) and 31 (β) kDa. Using the cross-linking reagent, disuccinimidyl suberate, ^{125}I-ChTX was specifically incorporated into a polypeptide of approximately 31 kDa. Cross-linking and binding of ^{125}I-ChTX to the purified ChTX receptor was inhibited by ChTX, iberiotoxin (IbTX), and tetraethylammonium (TEA). Liposomes containing the purified ChTX receptor were incorporated into planar lipid bilayers. In symmetric 150 mM KCl, the channels observed were >20-fold more selective for potassium over sodium and exhibited a large, single-channel conductance of 323 ± 2.5 pS in charged lipids and 249 ± 7 pS in neutral lipids. Depolarizing membrane potentials increased the open probability of the purified channels e-fold per 11.5 ± 0.3 mV, while intracellular calcium increased the open probability according to a third power (2.9 ± 0.2) relationship. Mean channel closed durations decreased while mean open times slightly increased as membrane potential and calcium concentration were elevated. The distributions of open and closed durations were well described by the sums of three and five to six exponential components, respectively. Purified maxi-K channels were blocked with micromolar affinity by external TEA and with nanomolar affinity by extracellular IbTX and ChTX. Kinetics of ChTX block of the purified channel revealed an equilibrium dissociation constant for toxin block of 4.6 ± 0.7 nM under conditions of physiological ionic strength. The purified maxi-K channel displays many of the biophysical and pharmacological properties of maxi-K channels derived from native tissue.

Potassium channels are integral membrane proteins that catalyze the passive transmembrane flow of potassium ions. Opening potassium channels tends to lower the excitability of a cell by hyperpolarizing the membrane potential. Calcium-activated potassium (K_{Ca})[1] channels are a special class of potassium channel that couples membrane excitability to intracellular calcium levels. These channels are found in numerous cell types and may regulate a broad range of functions. They regulate neurotransmitter release, secretion in endocrine and exocrine cells (Maruyama et al., 1983a,b; Petersen & Maruyama, 1984), myogenic tone in arterial smooth muscle (Brayden & Nelson, 1992), and contraction of tracheal (Brayden & Nelson, 1992; Jones et al., 1990, 1993) and taenia coli (Banks et al., 1979; Maas & Den Hertog, 1979) smooth muscle. The specific roles of different K_{Ca} channels are determined by how rapidly potassium ions diffuse through the channel and how this movement of potassium is regulated or gated. Some K_{Ca} channels are gated only by intracellular calcium while others are synergistically gated by calcium and voltage.

Large-conductance calcium-activated potassium (maxi-K) channels are a large group of K_{Ca} channels whose gating is regulated by both calcium and voltage (Barrett et al., 1982). Both depolarizing membrane potentials and high levels of intracellular calcium open maxi-K channels. Maxi-K channels must, therefore, contain structures that underlie both voltage-dependent and ligand-activated channel gating. This dual regulation of maxi-K channels by calcium and voltage distinguishes them from many other potassium channels and suggests that they may regulate membrane excitability in cells where calcium enters the cell through voltage-operated pathways.

† M.G.-C. is the recipient of a Fulbright Fellowship. H.-G.K. is supported by Erwin Schrodinger Fellowships P-0574-MED and P-0795-MED from the Austrian Research Foundation and by the APART program from the Austrian Academy of Sciences.

* To whom reprint requests should be addressed.

‡ Temple University School of Medicine.

§ Merck Research Laboratories.

⊗ Abstract published in *Advance ACS Abstracts,* November 15, 1995.

[1] Abbreviations: $Ca_{1/2}$, concentration of calcium giving half-maximal activation of the channel; ChTX, charybdotoxin; *hslo*, human maxi-K channel clone; DSS, disuccinimidyl suberate; IbTX, iberiotoxin; K_{Ca}, calcium-activated potassium channels; K_d, equilibrium dissociation constant for toxin; k_{off}, first-order toxin dissociation rate constant; k_{on}, second-order toxin association rate constant; *mslo*, mammalian maxi-K channel clone; maxi-K, large-conductance, calcium-activated potassium channels; ^{125}I-ChTX, monoiododinated ChTX; POPE, 1-palmitoyl-2-oleoylphosphatidylethanolamine; POPS, 1-palmitoyl-2-oleoylphosphatidylserine; POPC, 1-palmitoyl-2-oleoylphosphatidylcholine; P_o, open probability; SDS−PAGE, sodium dodecyl sulfate−polyacrylamide gel electrophoresis; TEA, tetraethylammonium; $V_{1/2}$, midpoint potential for activation of the channel; WGA, wheat germ agglutinin.

0006-2960/95/0434-15849$09.00/0

Electrophysiological studies have revealed substantial diversity in the properties of maxi-K channels. The single-channel conductance of maxi-K channels, which reflects intrinsic potassium permeability, varies from 90 to 350 pS (Latorre, et al., 1989). Even greater variability has been observed for the calcium sensitivity of maxi-K channel gating. Differences in calcium sensitivity range over about 3 orders of magnitude (McManus, 1991). In addition, differences in the inactivation properties of maxi-K channels are evident. Many voltage-gated potassium channels exhibit a time-dependent inactivation which occurs on the millisecond time scale. In contrast, most maxi-K channels do not inactivate. Rather they gate continuously in the presence of a calcium or voltage stimulus. However, a maxi-K channel from rat adrenal chromaffin cells was recently identified which rapidly inactivates, within milliseconds, after a step depolarization (Solaro & Lingle, 1992). The gating of maxi-K channels is also differentially controlled by regulatory enzymes. In rat brain plasma membrane, different maxi-K channel subtypes have been identified which exhibit striking differences in their gating and in their regulation by phosphatases and kinases (Reinhart et al., 1989). Thus, electrophysiological data points to a family of related types of maxi-K channels.

Recently, the genes that encode the pore forming α-subunits of maxi-K channels from invertebrate (Adelman et al., 1992; Atkinson et al., 1991) and mammalian tissues (Butler et al., 1993; Dworetzky et al., 1994; Pallanck & Ganetzky, 1994; Tseng-Crank et al., 1994) have been cloned and expressed in *Xenopus* oocytes. The deduced sequences of these cloned channels suggest a large diversity in maxi-K channel subtypes, which is consistent with the functional diversity described above. The mammalian maxi-K channel clones derived from mouse (*mslo*) and human (*hslo*) encode proteins of ~1200 amino acids with 10 hydrophobic, putative membrane-spanning regions (S1−S10). The first six membrane-spanning regions, S1−S6, are likely to form the pore of the channel as they are homologous to the six membrane-spanning regions that are found in the extended family of voltage-gated potassium channels (Jan & Jan, 1992). The *mslo* gene contains two potential RNA splice junctions and variable N-terminal domains (Butler et al., 1993), and the human gene contains four or more possible splice sites (Dworetzky et al., 1994; Pallanck & Ganetzky, 1994; Tseng-Crank et al., 1994). Expression studies have revealed functional differences between splice variants (Adelman et al., 1992; Tseng-Crank et al., 1994), providing a molecular basis for some of the diversity of expressed maxi-K channel subtypes. In addition, the β-subunit of the maxi-K channel has been cloned from bovine smooth muscle (Knaus et al., 1994b) and has been shown to modify the gating and pharmacology of expressed *mslo* α-subunits (McManus et al., 1995). Regulated expression of β-subunits of the maxi-K channel may further contribute to the diversity of expressed maxi-K channel subtypes.

Purification of the maxi-K channel presents the opportunity to identify the protein components that are associated with this channel in a specific tissue. The peptide toxin, charybdotoxin (ChTX), is a high-affinity blocker of the mammalian maxi-K channel which, in its monoiodinated form (^{125}I-ChTX), binds to a single class of sites in bovine aortic smooth muscle (Vazquez et al., 1989). Recently, a functional maxi-K channel subtype was purified to homogeneity from bovine tracheal smooth muscle (Garcia-Calvo et al., 1994). The purified protein consisted of two subunits, α and β, with apparent molecular weights of 62 and 31 kDa, respectively. Reconstitution of the purified protein into planar lipid bilayers revealed the presence of functional maxi-K channels. However, a detailed investigation into the permeation, gating, and pharmacological properties of the purified, reconstituted maxi-K channel was not done. To examine the molecular identity of tissue-specific maxi-K channel subtypes, we report here the purification and detailed characterization of the functional properties of the maxi-K channel from bovine aortic smooth muscle.

EXPERIMENTAL PROCEDURES

Materials. *Leiurus quinquestriatus* var. *hebraeus* venom was obtained from Alomone Labs, Jerusalem, Israel, and *Buthus tamulus* venom was purchased from Sigma. Na^{125}I was obtained from DuPont NEN. Recombinant *N*-glycanase was bought from Genzyme. Wheat germ agglutinin (WGA)-Sepharose was from Pharmacia LKB Biotechnologies Inc. Digitonin special grade (water soluble) was obtained from Biosynth AG, GF/C glass fiber filters were from Whatman, and L-α-phosphatidylcholine (type X-E) was from Sigma. The protein−gold reagent was from Integrated Separation Systems.

1-Palmitoyl-2-oleoylphosphatidylethanolamine (POPE), 1-palmitoyl-2-oleoylphosphatidylserine (POPS), and 1-palmitoyl-2-oleoylphosphatidylcholine (POPC) were purchased from Avanti Polar Lipids, Inc. (AL). Decane from Fisher Scientific, Inc., was of 99.9% mol purity. Bilayer cuvettes and chambers were purchased from Warner Instrument Corp. (CT). All other reagents were obtained from commercial sources and were of the highest purity commercially available.

Protein Purification and Characterization. Purification and Iodination of Toxins. ChTX and IbTX were purified from venom of the scorpions *L. quinquestriatus* var. *hebraeus* and *B. tamulus* as previously described (Galvez et al., 1990; Gimenez-Gallego et al., 1988). ChTX was iodinated as previously described (Vazquez, et al., 1989).

Preparation of Bovine Aortic Smooth Muscle Sarcolemmal Membrane Vesicles. Highly purified sarcolemmal membrane vesicles derived from bovine aortic smooth muscle were prepared as previously outlined (Vazquez et al., 1989). Membranes were resuspended in 160 mM NaCl, 20 mM Tris-HCl, pH 7.4, frozen in liquid N_2, and stored at −70 °C.

Purification of the ChTX Receptor from Bovine Aortic Smooth Muscle. The ChTX receptor was purified from bovine aortic smooth muscle using similar procedures to those previously reported for the purification of the tracheal smooth muscle ChTX receptor (Garcia-Calvo et al., 1994). In brief, membranes were solubilized at 4 °C, after six consecutive exposures to 1% digitonin. All buffers employed for solubilization and in subsequent purification steps contained 1 mM iodoacetamide, 0.1 mM phenylmethylsulfonyl fluoride, and 0.1% digitonin. After centrifugation at 180 000*g*, the resulting supernatants were incubated batchwise with WGA-Sepharose and the bound material specifically eluted with 5% *N*-acetyl-D-glucosamine. The sample was subsequently applied to a MonoQ HR 10/10 (Pharmacia) ion exchange column and eluted with a linear NaCl gradient. The active fractions were loaded on a Bio-Gel HPHT (Bio-

Rad) hydroxylapatite column and eluted with a sodium phosphate gradient. The fractions containing ^{125}I-ChTX binding activity were dialyzed, concentrated, and separated on a 7%−25% continuous sucrose density gradient. The active fractions were applied to a second continuous sucrose density gradient as described above. Fractions containing ^{125}I-ChTX binding activity were quickly frozen in liquid N_2 and stored at −70 °C.

Binding Assays. The interaction of ^{125}I-ChTX with bovine aortic sarcolemmal membrane vesicles or solubilized receptor was monitored as previously described (Garcia-Calvo et al., 1991; Vazquez, et al., 1989).

Cross-Linking Experiments. Fractions from the last sucrose density gradient centrifugation step were incubated with 90 pM ^{125}I-ChTX in a medium consisting of 10 mM NaCl, 10 mM TAPS-NaOH, pH 9.0, 5 μM paxilline, 0.05% digitonin, for 2 h at room temperature. The reaction was adjusted to 300 mM NaCl, and then disuccinimidyl suberate (DSS) was added to a final concentration of 0.18 mM. After being incubated at room temperature for 1 min, the reaction was stopped by addition of Tris-HCl, pH 7.4, up to a final concentration of 200 mM. Samples were dialyzed against 10 mM Tris-HCl, pH 7.4, 0.05% digitonin, concentrated 10-fold, and subjected to SDS−PAGE using 12% gels. Gels were dried and exposed to Kodak XAR film at −70 °C for 48 h.

Enzymatic Deglycosylation of the ^{125}I-ChTX-Cross-Linked β Subunit. Samples were prepared as indicated above and denatured by heating for 5 min at 95 °C in the presence of 0.5% SDS, 50 mM β-mercaptoethanol. Samples were diluted to a final SDS concentration of 0.15%, adjusted to 1.3% Nonidet P-40, and deglycosylation was started by addition of 2 IU of recombinant *N*-glycanase. After incubation at 37 °C for different periods of time, the reaction was stopped by addition of boiling SDS−PAGE sample buffer. Samples were subjected to SDS−PAGE using 12% gels, and dried gels were exposed to Kodak XAR-5 film.

Reconstitution of the ChTX Receptor into Liposomes. Aliquots of purified ChTX receptor in 0.05% digitonin were reconstituted into L-α-phosphatidylcholine liposomes as outlined previously (Garcia-Calvo et al., 1994). Proteoliposomes were resuspended into 100 mM NaCl, 20 mM Hepes-NaOH, pH 7.4, frozen in liquid N_2, and stored at −70 °C.

Polyacrylamide Gel Electrophoresis. Samples were resuspended into SDS−PAGE sample buffer containing 1% β-mercaptoethanol or 100 mM DTT and incubated at 37 °C for 120 min. Samples were subjected to SDS−PAGE and visualized by silver staining.

Protein Determination. Protein concentration was determined using either the Bradford (1976) or the Gold method (Stoschek, 1987) with bovine serum albumin as the protein standard.

Planar Lipid Bilayers. Planar lipid bilayers were formed in aqueous solution by painting lipids (50 mg/mL in decane) across a 0.25 mm aperture in a polystyrene partition. The lipids were composed of either POPE and POPS in a 1:1 molar solution or, where specifically noted, of POPE and POPC in a 7:3 molar ratio. Liposomes containing the purified ChTX receptor or native sarcolemma membranes were fused with the bilayer in the presence of an osmotic gradient which typically consisted of 150 mM KCl on the *cis* side and 10 mM KCl on the *trans* side. Occasionally, the osmotic gradient was 1 M KCl (*cis*):10 mM KCl (*trans*). The exact buffer composition is described in the figure legends. Proteoliposomes were added to the *cis* side, and the osmotic gradient was collapsed after a channel was observed. After fusion with the bilayer, the orientation of maxi-K channels was determined by their voltage and calcium sensitivity. Current and voltage are expressed in the normal electrophysiological convention. Voltage is referenced to the extracellular side of the channel, and current flowing from the inside to the outside is plotted in the positive direction. Single-channel currents were recorded onto tape with a video cassette recorder and a VR10 digital data recorder (Instrutech Corp., NY). For analysis of single-channel current amplitude, open probability, or open and closed durations, records were played into either a DEC 11/73 (Digital Equipment Corp., MA) or a Quadra 700 (Apple Computer Corp.) with an ITC16 interface (Instrutech Corp., NY).

RESULTS

Purification and Subunit Composition of the Bovine Aortic ChTX Receptor. The ChTX receptor from bovine aortic smooth muscle has been purified to apparent homogeneity using ^{125}I-ChTX binding as a marker. The overall procedure is similar to that previously described for the purification of the maxi-K channel from bovine tracheal smooth muscle (Garcia-Calvo, et al., 1994). The final preparation was enriched ~2000-fold relative to the crude solubilized material with a specific activity of ca. 1 nmol of ^{125}I-ChTX binding sites/mg of protein. ^{125}I-ChTX exhibits a high-affinity interaction with the purified preparation that is biochemically and pharmacologically indistinguishable from native aortic sarcolemmal membrane vesicles. The purified preparation displays an equilibrium dissociation constant for ^{125}I-ChTX of 25 pM under the low ionic strength conditions of the media (10 mM NaCl), not shown. Pharmacological agents such as native ChTX, IbTX, TEA, K^+, Ba^{2+}, and Ca^{2+} specifically inhibited binding of ^{125}I-ChTX to the purified preparation. The inhibition constants obtained were similar to those previously determined for native membranes (Vazquez et al., 1989).

To determine the subunit composition of the purified ChTX receptor, we analyzed fractions from the final sucrose density gradient centrifugation for their molecular weight composition (not shown). The highest specific activity for ^{125}I-ChTX binding appeared in two fractions that migrated with an apparent sedimentation coefficient of 22 S. Silver staining, after SDS−PAGE of fractions from the gradient, revealed that ChTX binding activity commigrated with a protein of apparent molecular weight of 65 000. Figure 1 shows the results of these experiments for the fraction with the highest ^{125}I-ChTX specific binding. Thus, the purified ChTX receptor minimally contains a major protein component with an apparent molecular weight of 65 kDa.

It has been previously shown that in both native and solubilized aortic membrane preparations ^{125}I-ChTX can be covalently incorporated into a protein of 31 000 Da that appears to be associated with the ChTX receptor (Garcia-Calvo et al., 1991). A protein with similar characteristics has been identified in the purified tracheal maxi-K channel preparation and has been shown to have functional properties (Garcia-Calvo et al., 1994).

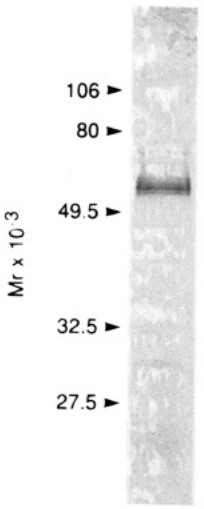

FIGURE 1: SDS−PAGE of purified ChTX receptor from bovine aortic smooth muscle. The fraction from the second sucrose density gradient centrifugation with the highest specific ^{125}I-ChTX binding activity (fraction 15, Figure 2) was subjected to SDS−PAGE as described under Experimental Procedures. Protein was visualized after silver staining. The migration of molecular weight standards is indicated by the arrows.

To determine whether the 31 kDa protein is also part of the purified ChTX receptor from aortic smooth muscle, we cross-linked ^{125}I-ChTX to the purified ChTX receptor using the bifunctional cross-linking reagent, disuccinimidyl suberate. Figure 2 shows that the distribution of specific ^{125}I-ChTX binding across the final sucrose density gradient exactly correlates with the covalent incorporation of ^{125}I-ChTX into the 31 kDa component. The incorporation of ^{125}I-ChTX into this component was abolished in the presence of inhibitors of the binding reaction, such as native ChTX, IbTX, TEA, K^+, and aflatrem, but was enhanced by paxilline, a stimulator of toxin binding (not shown).

When the purified ChTX receptor was cross-linked with ^{125}I-ChTX and then treated with *N*-glycanase, there was a time-dependent conversion of the 31 kDa protein into an intermediate form and a final product with apparent molecular weights of 26 and 21 kDa, respectively (not shown). Thus, the purified ChTX receptor contains a 31 kDa protein that is heavily glycosylated and is the acceptor for covalent incorporation of ^{125}I-ChTX. These data indicate that a purified preparation of the bovine aortic smooth muscle ChTX receptor migrates as a large particle and appears to consist of two subunits, 65 and 31 kDa, after denaturation of the preparation in the presence of reducing agents.

Functional Properties of the Purified ChTX Receptor. The Purified ChTX Receptor is a High-Conductance K^+ Selective Channel. We tested whether the protein components associated with the ChTX receptor are sufficient to form fully functional maxi-K channels by incorporating the purified ChTX receptor into planar lipid bilayers. Fusion of proteoliposomes containing the purified ChTX receptor with planar lipid bilayers resulted in the appearance of large, single-channel cationic currents. The magnitude and direction of these currents followed the predicted equilibrium potential for potassium (Figure 3). Part A of the Figure 3 shows a single purified channel in a bilayer held at −10 mV with 150 mM KCl on the inside. When KCl on the outside was raised from 10 to 50 and 150 mM, current amplitudes of 14, 4, and −3.5 pA were observed. A more quantitative

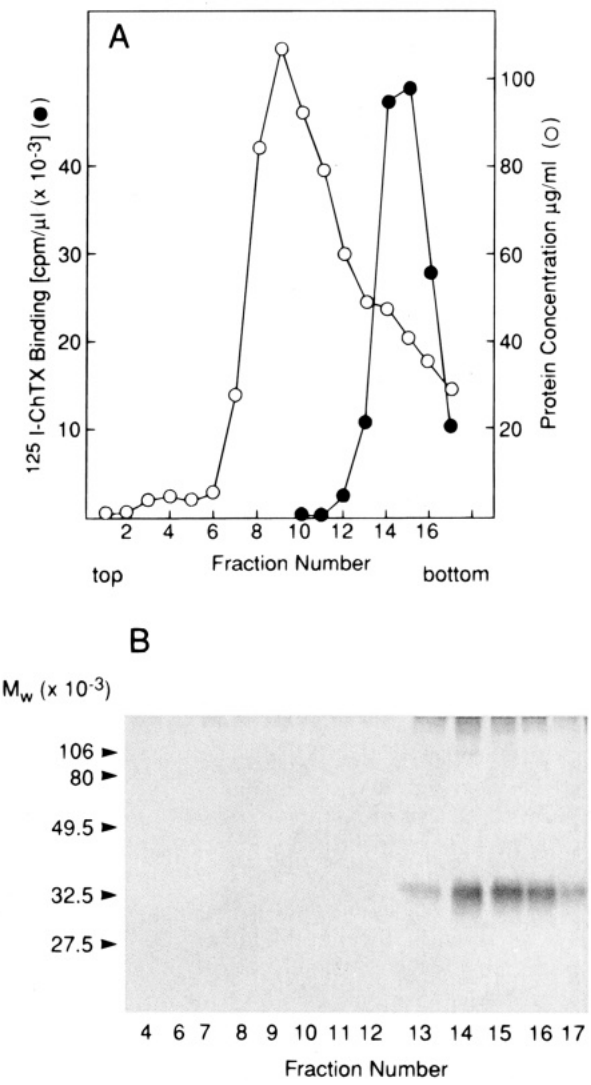

FIGURE 2: Cross-linking of ^{125}I-ChTX to purified bovine aortic ChTX receptor. (A) Sucrose density gradient centrifugation. Fractions from the last sucrose density gradient centrifugation were analyzed for protein content (○) and ^{125}I-ChTX binding activity (●) as indicated under Experimental Procedures. (B) ^{125}I-ChTX cross-linking. Fractions from A were cross-linked with ^{125}I-ChTX in the presence of DSS, as indicated under Experimental Procedures. The migration of molecular weight standards is indicated by the arrows.

measure of the potassium selectivity of the purified ChTX receptor is shown in Figure 3B. Plots of the single-channel current amplitude as a function of membrane potential reveal that when the concentration of potassium on the outside was raised from 10 to 150 mM, the reversal potential shifts to more positive values. The single-channel currents approach 0 pA at membrane potentials of 0.6, −24, and −57 mV when the potassium on the outside is 150, 50, and 10 mM, respectively. These values are very close to the predicted reversal potential values for potassium of 0, −24, and −56 mV, suggesting that the purified ChTX receptor is highly selective for potassium over chloride.

In addition to its capacity for discrimination between K^+ and Cl^-, the maxi-K channel allows very rapid rates of K^+ transmembrane diffusion. The single-channel conductance provides a measure of the net rate of K^+ movement through the channel. The plots of single-channel current vs membrane potential (Figure 3B) show that the purified ChTX receptor exhibits single-channel conductance values of ~300

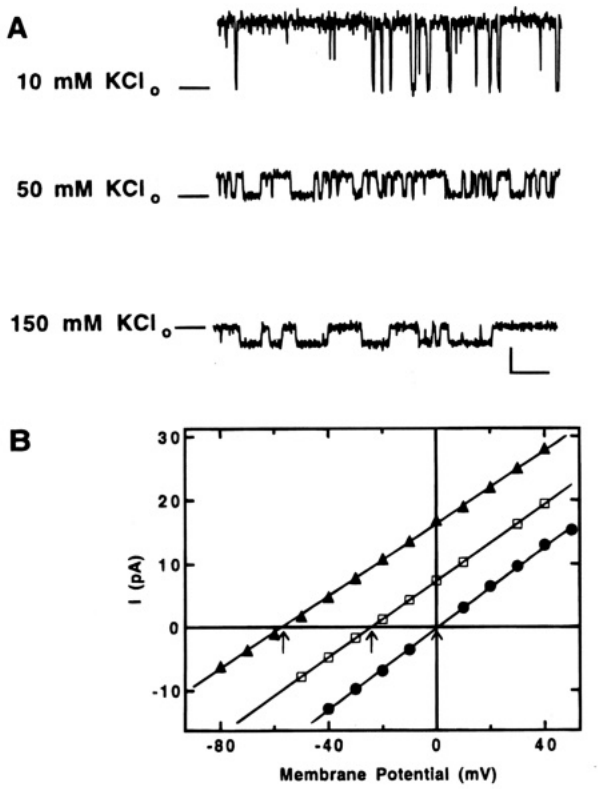

FIGURE 3: Cation selectivity of the purified ChTX receptor reconstituted into a planar lipid bilayer. (A) Currents through a single purified ChTX receptor at a membrane potential of −10 mV with 150 mM KCl on the inside and different concentrations of KCl at the outside. Currents were filtered at 300 Hz, and the vertical and horizontal scale bars represent 5 pA and 100 ms, respectively. The solid lines on the left indicate the closed channel current level. (B) Amplitudes of current through a single purified ChTX receptor are plotted as a function of membrane potential with 150 mM KCl on the inside and 10 (▲), 50 (□), and 150 (●) mM KCl on the outside. The lines represent the best fit of the data to a straight line: the slope represents the single-channel conductance, and the *x*-intercept represents the reversal potential. Values from the fits for conductance in picosemiens and reversal potential in millivolts were 285 and −57.2, respectively, at 10 mM KCl; 301 and −24.2 at 50 mM KCl; 320 and 0.59 at 150 mM KCl. The predicted reversal potentials for potassium, indicated by the arrows, were calculated based on potassium ion activity. A and B were obtained from the same purified channel incorporated into a bilayer composed of charged, POPS and neutral POPE lipids in a 1:1 molar ratio.

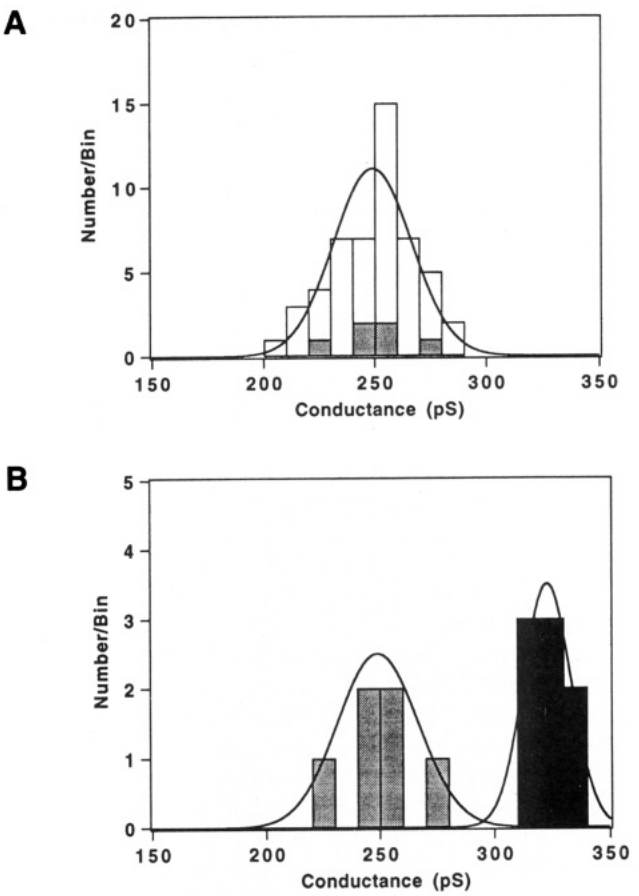

FIGURE 4: Comparison of single-channel conductance for the purified ChTX receptor and the native maxi-K channel. (A) Histogram of single-channel conductance values for the native (open bins) and purified (light grey bins) maxi-K channel when the bilayer contained only neutral lipids. The line represents the best fit of a Gaussian distribution to the single-channel conductance values for the native maxi-K channel with a mean of 249 pS and a standard deviation of 17 pS, $n = 51$. (B) Histogram of single-channel conductance for the purified maxi-K channel when the bilayer contains either the neutral zwitterionic lipids (light grey bins) or neutral and negatively charged lipids (dary grey bins). The lines represent the best fits of Gaussian distributions to the single-channel conductance values with mean and standard deviations of 249 ± 18.5 and 323 ± 7.2 pS for neutral and charged lipids, respectively. Bilayers containing only neutral lipids were composed of POPE and POPC in a 7:3 molar ratio. Those containing neutral and charged lipids were composed of POPE and POPS in a 1:1 molar ratio. Both sides of the bilayer contained 150 mM KCl, 10 mM Hepes pH 7.2, 3.5 mM KOH. Intracellular calcium levels ranged from 5 to 100 μM.

pS in the presence of negatively charged lipids. Thus, the purified ChTX receptor permits very rapid rates for transmembrane diffusion of K^+.

To compare the single-channel conductance of the purified ChTX receptor with that of the native maxi-K channel, we examined purified and native channels under conditions of identical lipid composition. Part A of Figure 4 plots histograms of single-channel conductance values determined for the purified ChTX receptor and for the native maxi-K channel when the bilayer was composed of neutral zwitterionic synthetic lipids. Under these conditions, with solutions of 150 mM KCl on both sides of the channel, the single-channel conductance values for the purified ChTX receptor and native maxi-K channel were nearly identical at 249 ± 7 ($n = 6$) and 249.2 ± 2.5 pS ($n = 51$), respectively. These values are clearly less than the 300 pS values derived from Figure 3 in which the purified ChTX receptor was incorporated into a bilayer that contained negatively charged lipids. This discrepancy can be entirely accounted for by differences in the lipid composition of the artificial planar bilayer. To examine the effect of charged lipids, we compared the single-channel conductance of the purified ChTX receptor under conditions where the bilayer is composed of either neutral zwitterionic lipids or a combination of negatively charged and neutral lipids. The histograms in part B of Figure 4 demonstrate that, in the presence of negatively charged lipids, the single-channel conductance of the purified ChTX receptor is shifted to much larger values, 323 ± 2.5 pS, than when the bilayer contains only neutral lipids, 249 ± 7 pS. Similar effects of charged lipids on conductance have been reported for the native maxi-K channel from skeletal muscle (Moczydlowski et al., 1985). These effects have been attributed to differences in surface charge density contributed by the head group of the lipid moiety. Thus, the purified ChTX receptor exhibits a high intrinsic K^+ permeability which

Table 1: Conductance of the Purified Maxi-K Channel under Conditions of Varied Potassium Concentration and Lipid Composition

lipid composition	$[KCl]_{cis}/[KCl]_{trans}$ (mM/mM)	conductance (pS)
POPE:POPC (7:3)	150/10	193.9 ± 2(3)
	150/150	249 ± 7(6)
POPE:POPS (1:1)	150/10	285(1)
	150/50	301(1)
	150/150	323 ± 2.5(8)
	1000/10	363(1)
	1000/100	400(1)

appears to be influenced by surface charge.

The conductance of potassium channels is generally influenced by the concentration of K^+ in the medium (Latorre & Miller, 1983). We examined the conductance of the purified maxi-K channel at different concentrations of potassium chloride in either charged or neutral lipids. Table 1 shows that as the concentration of K^+ is raised the single-channel conductance increases. A similar effect of K^+ on the single-channel conductance has been observed for maxi-K channels from skeletal muscle and is believed to result from the occupancy of K^+ binding sites within the pore of the channel (Blatz & Magleby, 1984; Vergara et al., 1984).

A remarkable feature of the maxi-K channel is that, in spite of its high permeability to K^+, its permeability to the smaller Na^+ ion is virtually undetectable. To determine whether the purified ChTX receptor is selectively permeant to potassium over sodium, we examined how the single-channel current amplitudes changed when extracellular potassium was replaced completely by sodium. The single-channel records in part A of Figure 5 show that the purified ChTX receptor carries a small inward current of −4 pA when the solutions on both sides of the bilayer contain 150 mM potassium and the membrane potential is −10 mV. When the potassium on the outside of the channel is replaced by 50 and 150 mM sodium, large outward currents of 7 and 5 pA are observed, respectively. The larger outward current observed in the presence of 50 mM NaCl can be attributed to surface charge effects resulting from differences in ionic strength on either side of the bilayer (MacKinnon et al., 1989). The relative permeability of the maxi-K channel to Na^+ and K^+ can be determined by examining single-channel currents as a function of membrane potential under bi-ionic conditions, as described above. Part B of Figure 5, reveals that, in the presence of extracellular sodium and intracellular potassium, no inward current is observed at large negative potentials, −90 and −60 mV for 50 and 150 mM sodium, respectively. This suggests that no detectable inward current was carried by sodium. The relative permeability of the purified ChTX receptor for sodium over potassium, determined from extrapolated reversal potentials, was approximately 0.06 and 0.03 for 150 and 50 mM sodium, respectively. Thus, as expected for the maxi-K channel, the purified ChTX receptor is highly selective for potassium over sodium.

The Purified ChTX Receptor is Gated by Calcium and Voltage. A special feature of the maxi-K channel is that its permeability to K^+ is synergistically regulated by the membrane potential and by intracellular calcium levels. Part A of Figure 6 shows single-channel records of a purified ChTX receptor in a bilayer composed of charged lipids at

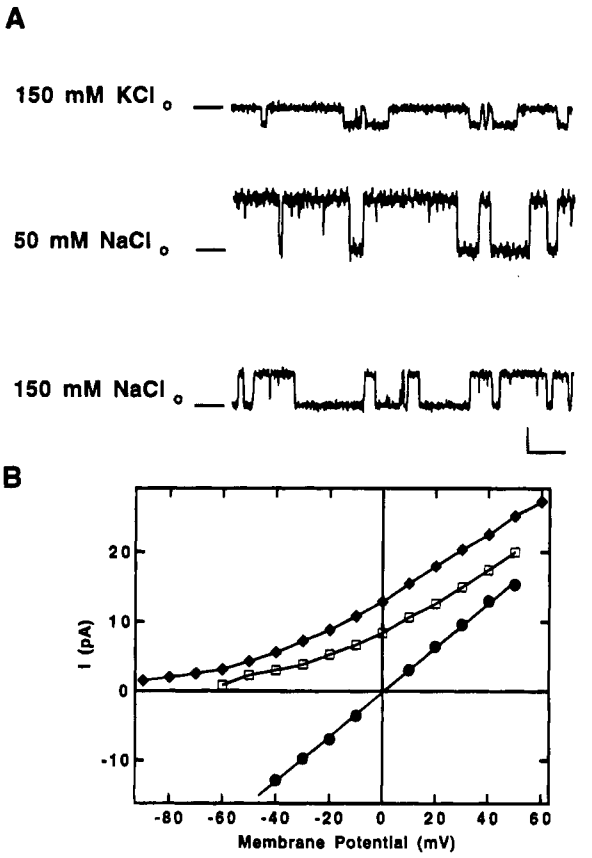

FIGURE 5: Selectivity of the purified maxi-K channel for K^+ over Na^+. (A) Currents through purified single maxi-K channels at a membrane potential of −10 mV when 150 mM KCl on the outside is replaced completely by 50 and 150 mM NaCl. Filtering and scale bars are as in Figure 3. The solid lines on the left side indicate the closed current level. (B) Amplitudes of single-channel current are plotted as a function of membrane potential when the extracellular solution contains 150 mM KCl (●), 50 (◆), or 150 (□) mM NaCl. For both A and B, solutions at the intracellular face of the channel contain 150 mM KCl.

two different voltages and concentrations of calcium at the cytoplasmic side. The fraction of time the channel spends in the open, K^+ conductive, state decreased from 0.34 to 0.017 as the membrane potential was hyperpolarized from −20 to −60 mV with 5 μM calcium on the inside. Increasing the intracellular calcium concentration from 5 to 9 μM increased the channel open probability from 0.017 to 0.034 at a constant membrane potential of −60 mV. Thus, the open probability of the purified ChTX receptor channel is regulated by both voltage and intracellular calcium.

To quantitate the calcium and voltage sensitivity of the purified ChTX receptor we examined changes in the open probability at several different membrane potentials and levels of calcium on the inside of the channel. The influence of membrane potential on channel open probability is shown for three different concentrations of intracellular calcium in part B of Figure 6. The family of curves at different calcium levels shows that channel open probability increased monotonically as the membrane potential was made more positive. The midpoint potential for activation ($V_{1/2}$) of each curve shifted to more negative values as the concentration of calcium was raised. The slopes of the curves for each calcium concentration were similar and reveal that channel open probability increased e-fold per 10−12 mV. The channel shown in Figure 6 was more sensitive to activation

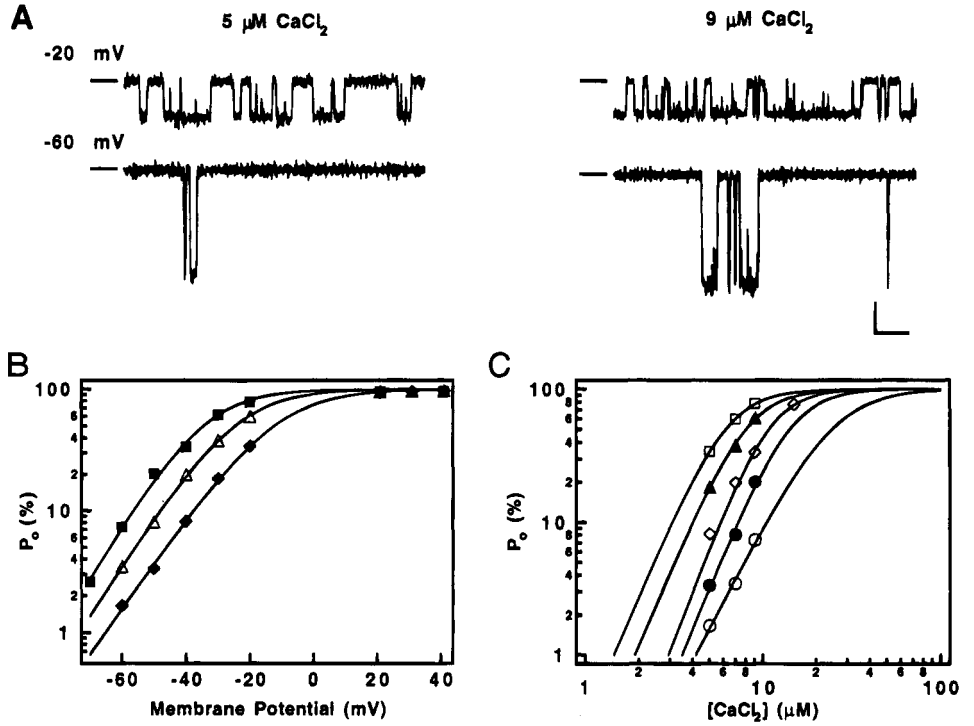

FIGURE 6: Calcium- and voltage-dependent gating of the purified maxi-K channel. (A) Currents through a single purified channel at different membrane potentials and concentrations of calcium at the inside. Filtering and scale bars are as in Figure 3. (B) Single-channel open probability (P_o), in percent, is plotted as a function of membrane potential when the intracellular calcium concentration is 5 (◆), 7 (△), and 9 (■) μM. The lines represent the best fit of the data to a Boltzmann equation where $P_o = 1/1 + \exp(V_{1/2} - V_m)/k$, V_m is membrane potential, $V_{1/2}$ is the midpoint potential for activation, and k is a slope factor. Values from the fits for $V_{1/2}$ (mV) and k (e-fold change per mV) are −12.3 and 11.5 at 5 μM Ca, −24.7 and 10.6 at 7 μM Ca, and −34.55 and 9.9 at 9 μM Ca. (C) Single-channel open probability, in percent, is plotted as a function of calcium concentrations at the inside when the membrane potential is −60 (○), −50 (●), −40 (◇), −30 (▲), and −20 (□) mV. The lines represent the best fit of the data to a Hill equation of the form $\log P_o/(1 - P_o) = n(\log [Ca] - \log Ca_{1/2})$ where n is the Hill coefficient and $Ca_{1/2}$ is the calcium concentration required for half-maximal activation. Values from the fits for $Ca_{1/2}$ (μM) and n are 24.5 and 2.6 at −60 mV, 14.2 and 3.3 at −50 mV, 11 and 3.1 at −40 mV, 8 and 3.2 at −30 mV, and 6.2 and 3.2 at −20 mV. A−C were obtained from the same purified channel incorporated into a bilayer composed of charged POPS and neutral POPE lipids in a 1:1 molar ratio. Solutions bathing both sides of the channel contained 150 mM KCl, 10 mM Hepes, 3.5 mM KOH, pH 7.2.

by calcium and voltage than was typical. In a total of five similar experiments, the average $V_{1/2}$ at 5 μM calcium was 20.6 ± 9.4 mV, while the open probability increased e-fold per 11.4 ± 0.47 mV. This slope factor is similar to the average value of 11.5 ± 0.32 mV obtained from 16 measurements at different calcium concentrations (5−70 μM). Thus, calcium permits the purified receptor to open more readily at negative voltages without affecting the slope of the voltage response function.

The membrane potential should also influence the calcium sensitivity of the maxi-K channel. Plots of channel open probability as a function of calcium, shown in part C of Figure 6, provide a means for examining the calcium binding reactions which lead to channel activation. The family of curves at different voltages shows that as the membrane potential was increased from −60 to −20 mV, the concentration of calcium giving half-maximal activation, $Ca_{1/2}$, decreased. When the membrane potential was held at −60 mV, the $Ca_{1/2}$ was 25 μM, while at a membrane potential of −20 mV, the $Ca_{1/2}$ was 6.2 μM. Thus, positive voltages increase the apparent calcium sensitivity for activation of the purified ChTX receptor. The slopes of these calcium activation curves give estimates of the minimum number of bound calcium ions required to cause channel opening. These slopes were similar for the voltages shown, ranging from 2.6 to 3.3. We have examined the influence of calcium on open probability at different voltages in three other experiments and found similar results. The average $Ca_{1/2}$ at −20 mV was 35 ± 19 μM (n = 3), and the Hill coefficient, averaged from several different voltages, was 2.9 ± 0.2 (n = 13) when solutions on both sides of the channel contained 150 mM KCl. Thus, the range of Hill slopes observed suggests that four or more calcium molecules can bind to the purified channel during maximal activation.

Gating Kinetics of the Purified ChTX Receptor. We examined the kinetic properties of single purified channels at various calcium concentrations. Figure 7 shows the effects of raising the internal calcium concentration on the open and closed durations of a channel held at −40 mV. Plots of sequentially averaged mean open vs mean closed times reveal that increasing the calcium concentration from 5 to 7 and then to 9 μM caused a clear decrease in the mean closed times from 201 to 48.4 to 25.4 ms, respectively. The mean open times were unchanged over this range of calcium concentrations (14.4, 15.0, and 14.5 ms). Thus, the primary effect of raising internal calcium on channel gating kinetics was to decrease channel closed times. This suggests that, at our level of resolution, most of the calcium-dependent gating transitions occur between closed states.

Figure 8 plots the distributions of open and closed time durations from the experiment shown in Figure 7 at 5, 7 and 9 μM calcium. The distributions of open times at each calcium concentration were well-described by the sums of three exponential components, and the closed times were fit

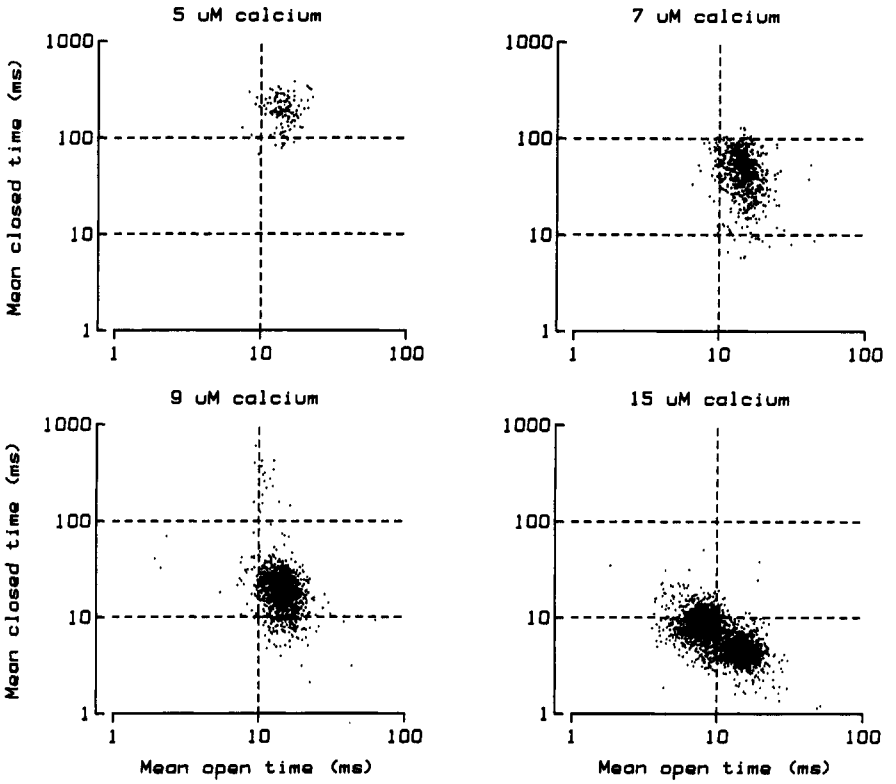

FIGURE 7: Effects of calcium on sequentially averaged mean open and mean closed times. Mean open and mean closed times were sequentially calculated for groups of 10 open and 10 closed event durations and plotted as individual points. Recording is from a single channel held at −40 mV and exposed to different calcium concentrations on the internal side. Filtering was 365 Hz. Solutions contained 150 mM KCl and 10 mM Hepes, pH 7.2, on both sides of the membrane.

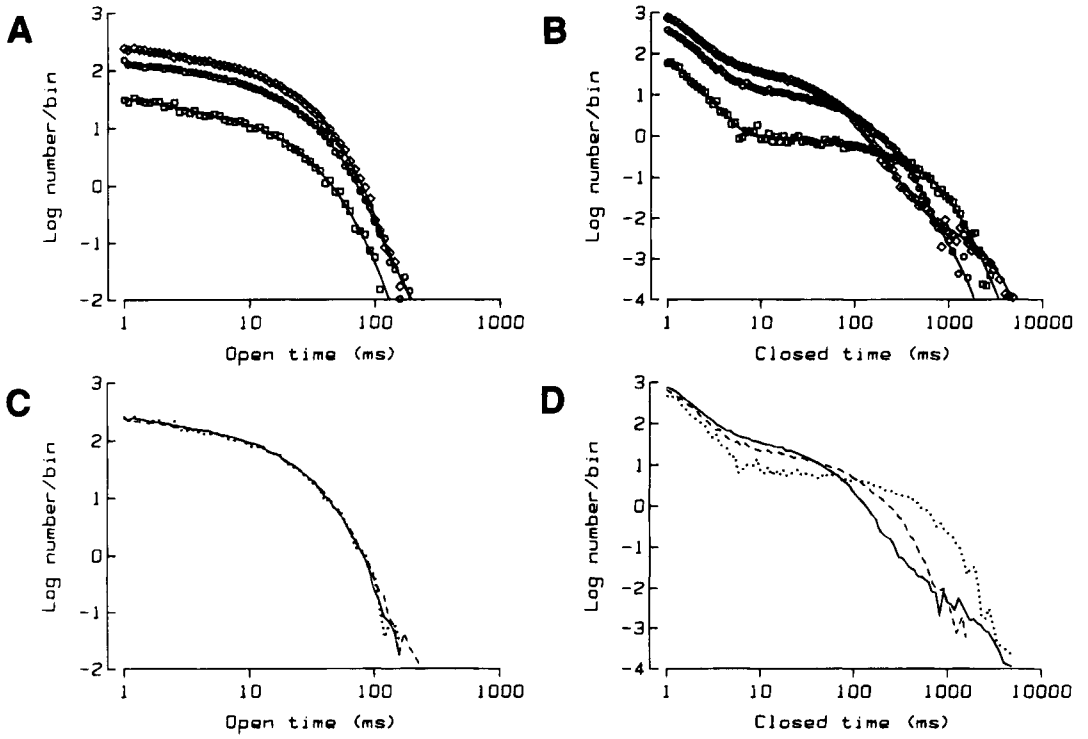

FIGURE 8: Effects of calcium on distributions of open and closed times. The distributions of open (A) and closed (B) times are plotted at 5 (□), 7 (○), and 9 (◇) μM calcium. The solid lines in A show fits to the open time distributions with the sums of three exponential components, and the lines in B show fits to the closed times with five exponential components. (C, D) Open and closed time distributions, respectively, after scaling the data at different calcium concentrations to contain the same number of events. In C and D, the dotted line shows the data obtained at 5 μM calcium, the dashed line shows the distribution at 7 μM calcium, and the solid line shows the distribution at 9 μM calcium. Filtering and experimental conditions are the same as for Figure 7.

with the sums of five components. At 9 μM calcium, a sixth closed-time component was detected with a mean duration of about 1 s, which probably reflects infrequent entries into an inactivated state. The number of components observed

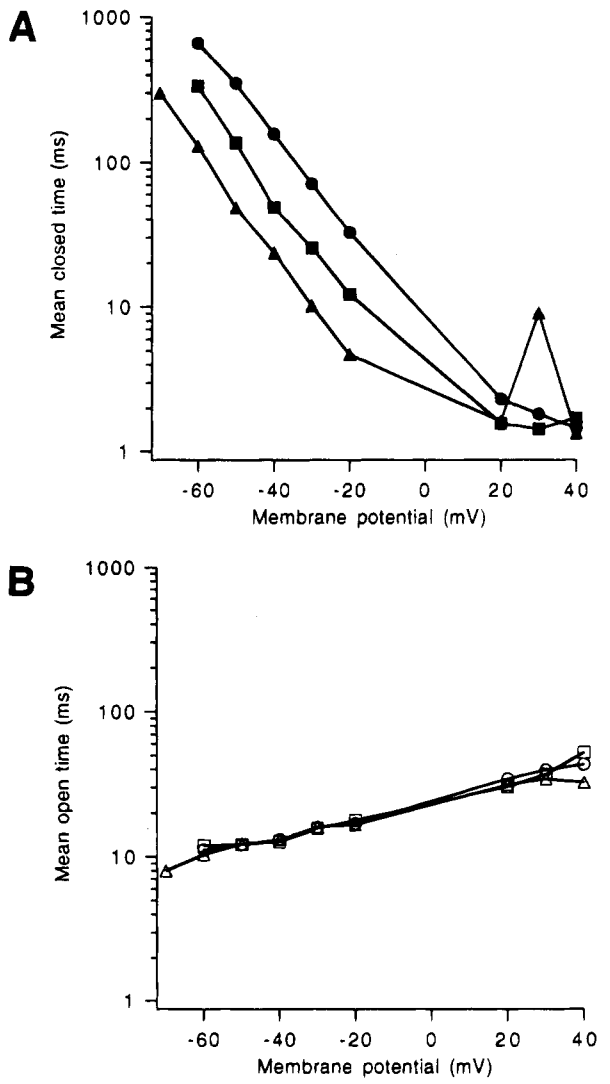

FIGURE 9: Effect of membrane potential on mean open and mean closed times. The mean closed (A) and mean open (B) times were determined for a single channel as a function of membrane potential at 5 (●, ○), 7 (■, □), and 9 (▲, △) μM calcium. Each determination was made from 2 to 5 min of data. Filtering was identical (0.45 kHz) for all conditions and was sufficient to exclude false events.

in the distributions of closed times are consistent with a channel that is gated by binding of four or more calcium ions. When the open and closed time distributions are scaled to contain equal numbers of events (Figure 8C,D), we can see that the open times were nearly identical at each calcium concentration while the closed times were clearly modified by calcium. Increasing calcium led to a reduction in probability of observing long closed times.

Figures 7 and 8 showed that the primary effect of calcium on the kinetics of channel gating was to decrease channel closed durations. Figure 9 shows that membrane depolarization also increases channel open probability by decreasing channel closed times. Mean channel closed times (Figure 9A) decreased exponentially as the membrane potential was increased until a minimal duration of 1−2 ms was reached at 20−40 mV. The flattening of the closed time vs membrane potential relation at depolarized potentials may reflect the emergence of a calcium- and voltage-independent closed state at high channel open probability (McManus & Magleby, 1991) or an inability to detect briefer closed events. The slopes of the exponential decline in mean closed times (average e-fold change per 12.8 ± 1.6 mV) were similar at each calcium concentration. These slopes were also similar to the slopes obtained from plotting channel open probability vs membrane potential (Figure 6). In contrast, the mean open times (Figure 9B) increased only slightly (e-fold increase per 321 ± 47 mV at different calcium concentrations) as the membrane potential was increased. Similar effects were seen in three other experiments, with one channel exhibiting a slightly larger sensitivity of channel open times to calcium and membrane potential. These effects of calcium and voltage on open and closed durations suggest that many of the voltage- and calcium-dependent transitions that control channel gating occur between closed states.

Modal Gating. We have observed modal gating with the purified maxi-K channel. At each of the three lower calcium concentrations shown in Figure 7, the mean open and closed times appeared to be grouped into a single population, suggesting homogeneous gating behavior. However, two distinct modes of gating behavior were seen at the highest calcium concentration of 15 μM. In the high open probability mode, the mean open time (15.0 ms) was similar to the open times observed at lower calcium concentrations, while the mean closed time decreased to 4.5 ms. During the low open probability mode, the mean open time was 8.1 ms while the mean closed time was 9.2 ms. Two observations suggest that the high open probability mode is the same as the gating mode observed at lower concentrations. The open times at low calcium and in the high open probability mode are the same. In addition, channel gating started in the high open probability mode when the calcium was raised from 9 to 15 μM. The low open probability mode data was due to two long sojourns from the high open probability mode. The occurrence of modal gating in a purified, reconstituted maxi-K channel suggests that this function is intrinsic to the channel protein and not due to modulation of the channel by other proteins.

The Purified Channel is Blocked by Tetraethylammonium and Peptide Toxins. Peptide toxin and organic cation blockers of K^+ channels provide the means to identify and categorize K^+ channel subtypes. Tetraethylammonium (TEA) is an organic cation which is known to block current through the maxi-K channel from the extracellular side with micromolar affinity (Blatz & Magleby, 1984; Yellen, 1984). Part A of Figure 10 shows that current through a single purified channel molecule is reduced by ~45% when 200 μM TEA is applied to the outside of the channel. Extracellular TEA block of the maxi-K channel is also weakly voltage-dependent (Villarroel et al., 1988). We examined the effect of voltage on TEA block by measuring single-channel current amplitude as a function of voltage in the presence of varying concentrations of TEA (Figure 10B). The voltage-dependence of TEA block is most apparent at the extreme membrane potentials and concentrations of TEA. Addition of 1 mM TEA caused a 77% reduction in the single-channel current amplitude when the membrane potential was 60 mV, while the current amplitude was reduced by 89% when the membrane potential was −60 mV. The equilibrium dissociation constant for TEA at 0 mV [$K_{TEA(0)}$] and the location of the TEA site within the membrane field was estimated using eq 1

$$i_{TEA} = i_0\left(1 + \frac{[TEA]}{K_{TEA(0)}e^{\left(-\partial V_m \frac{nF}{RT}\right)}}\right)^{-1} \quad (1)$$

where i_0 and i_{TEA} represent the single channel current amplitude in the absence and presence of extracellular TEA, V_m represents the membrane potential, z represents the valence of TEA, and ∂V_m represents the fraction of the voltage drop sensed at the TEA site measured from the extracellular side of the membrane. The fit to eq 1 for each concentration of TEA provided a good description of the data with an average $K_{TEA(0)}$ value of 193 ± 4 μM and an average ∂ value of 0.186 ± 0.007. Thus, extracellular TEA blocks the purified channel with micromolar affinity at a site which is located approximately 19% across the membrane dielectric from the outside.

The molecular identity of the maxi-K channel from aortic smooth muscle is also defined by its high-affinity interactions with the peptide toxins ChTX and iberiotoxin (IbTX). The kinetics of IbTX (Giangiacomo et al., 1992, 1993) and ChTX (Anderson et al., 1988; MacKinnon & Miller, 1988) block of the maxi-K channel are well-established and provide a stringent test of its molecular identity. We examined the interaction of both IbTX and ChTX with single purified maxi-K channels incorporated into lipid bilayers. Addition of 10 nM IbTX to the extracellular side caused the appearance of long, nonconducting silent periods of approximately 10 min in duration which were interrupted by periods of normal channel activity (not shown). These long nonconducting silent periods are typical of IbTX blocking the maxi-K channel (Giangiacomo et al., 1992). ChTX block of the native smooth muscle maxi-K channel is characterized by much shorter blocked periods of ~60 s in duration (Giangiacomo et al., 1993). Since the shorter blocked periods observed with ChTX are more amenable to analysis of toxin blocking kinetics, we examined ChTX block of the purified maxi-K channel in detail. Part A of Figure 11 shows that addition of 5 nM ChTX to the extracellular side of the purified channel resulted in the appearance of nonconducting silent periods, ~30 s in duration, which were interrupted by apparently normal periods of channel activity. Increasing the concentration of ChTX to 15 nM increased the frequency of the silent periods but not their duration. This pattern of block is consistent with the bimolecular mechanism for ChTX block of the maxi-K channel from skeletal muscle (Anderson et al., 1988) in which the silent periods represent times when toxin is bound to the channel and are related to the first-order dissociation rate constant, k_{off}. The unblocked periods represent times when toxin is not bound to the channel and are related to the pseudo-first-order association rate constant, k_{on}[ChTX]. It follows from this mechanism that the distributions of the blocked and unblocked times should follow single exponentials where the time constant for blocked durations is equal to $1/k_{off}$ and the time constant for the unblocked durations is equal to $1/k_{on}$[ChTX]. In addition, the time constant for block should be independent of toxin concentration, while the time constant for unblock will decrease with increasing concentrations of ChTX. Part B of Figure 11 shows that the distributions for the blocked and unblocked durations are best described by single-exponential components. The time constants for the blocked durations at 5 and 15 nM ChTX, 20 and 18 s, respectively,

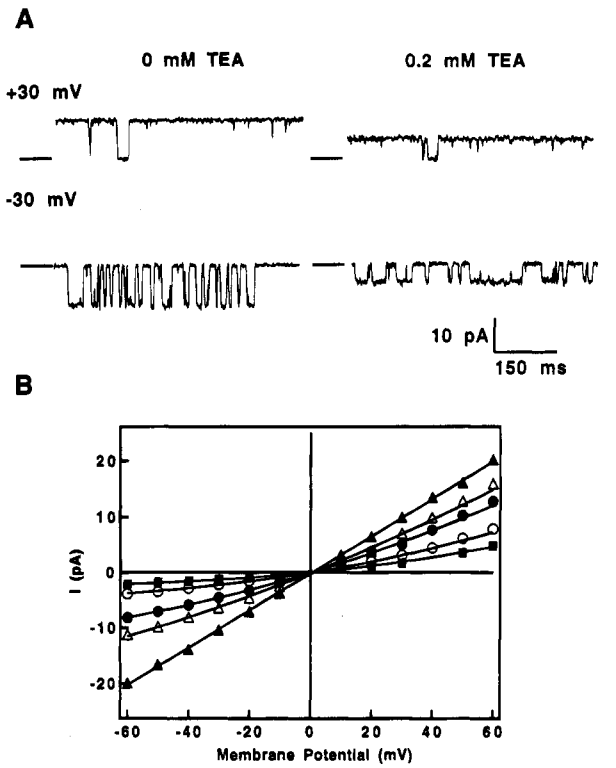

FIGURE 10: Block of the purified maxi-K channel by tetraethylammonium ion. (A) Currents through a single channel at different membrane potentials and different concentrations of TEA added to the outside of the channel. Currents were filtered at 200 Hz. (B) Single-channel current amplitude is plotted as a function of membrane potential when the extracellular concentration of TEA (mM) is 0 (▲), 0.1 (△), 0.2 (●), 0.5 (○), and 1.0 (■). The lines represent the best fit of the data to eq 1. A and B were obtained from the same purified channel incorporated into a bilayer composed of charged POPS and neutral POPE lipids in a 1:1 molar ratio. Solutions bathing both sides of the channel contained 150 mM KCl, 10 mM Hepes, 3.5 mM KOH, pH 7.2.

are similar. In contrast, the time constants for the unblocked durations decreased from 22 to 5.9 s as the ChTX concentration was raised 3-fold. The time constants for toxin block and unblock derived from Figure 11 provide a means for calculating the ChTX equilibrium dissociation constant (K_d) where K_d(M) = k_{off} (s^{-1})/k_{on} (M^{-1} s^{-1}). The K_d for ChTX block of the purified channel, calculated in this way from the kinetics in Figure 11B, is 5 nM. We examined ChTX block of the purified channel in four separate experiments where KCl on both sides of the channel was 150 mM and the membrane potential was +40 mV. Under these conditions, the average K_d value for ChTX block of the purified channel in lipid bilayers was 4.6 ± 0.7 nM (Table 2). This value is significantly weaker than the K_d value obtained from binding of ^{125}I-ChTX to the purified ChTX receptor under low ionic strength conditions. The kinetics of ChTX binding to and unbinding from the maxi-K channel are strongly dependent on the concentrations of salt on either side of the channel (Anderson et al., 1988; MacKinnon & Miller, 1988). In order to compare K_d values obtained from bilayer experiments with K_d values obtained from ^{125}I-ChTX binding, we examined the kinetics of ChTX block of the purified channel under conditions of varying ionic strength on the outside. Table 2 shows the ChTX dissociation and association rate constants and the calculated K_d values at different concentrations of KCl on the outside of the channel. Under

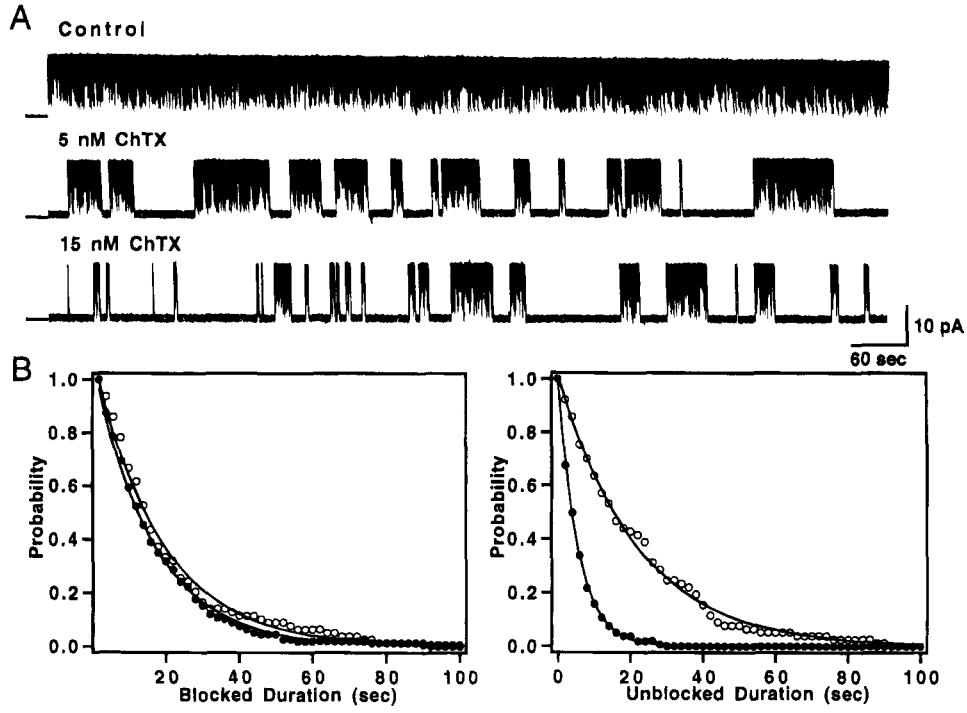

FIGURE 11: Charybdotoxin block of the purified maxi-K channel. (A) Currents through a single purified channel at different concentrations of ChTX added to the extracellular side of the channel were filtered at 60 Hz. The durations of blocked (B) and unblocked (C) events in 5 (O) and 15 (●) nM ChTX are plotted as cumulative dwell-time distributions. The lines plot single-exponential fits to the data. The time constants for blocked durations at 5 and 15 nM are 20 and 18 s, respectively. Time constants obtained for the unblocked durations are 22 and 5.9 s at 5 and 15 nM ChTX, respectively. The distributions for 5 and 15 nM ChTX were constructed from 76 to 157 events, respectively. The composition of the lipid bilayer is as described in Figure 3. Conditions: 150 mM KCl, 10 mM HEPES, pH 7.2 inside and outside, 150 μM $CaCl_2$ inside, 60 μg of BSA/mL outside, +40 mV.

Table 2: Kinetics of ChTX Block of the Purified Maxi-K Channel[a]

$[KCl]_o$ (mM)	V_m (mV)	k_{off} (s^{-1})	k_{on} (M^{-1} s^{-1})	K_d (nM)
10	0	0.052	5.9×10^8	0.087
150[b]	+40	0.034 ± 0.007	$(7 \pm 1) \times 10^6$	4.6 ± 0.7
187[c]	+40	0.035	2.5×10^6	14.1

[a] The concentration of KCl on the inside was 150 mM, and the bilayer contained the lipids POPE:POPS in a 1:1 molar ratio. [b] Blocking kinetics were determined from four different channels with the number of toxin-blocked events for each channel ranging from 66 to 234. [c] Blocking kinetics were determined from a single channel at four different concentrations of ChTX with an average of 59 toxin-blocked events detected for each condition.

conditions of low ionic strength on the outside, the K_d value for ChTX block of the purified channel was 87 pM when the external KCl concentration was 10 mM. Thus, under conditions of physiological ionic strength ChTX blocks current through the purified channel with nanomolar potency, while under low ionic strength conditions ChTX blocks with picomolar potency.

DISCUSSION

Electrophysiological studies have revealed significant variation between maxi-K channels from different tissues. The single-channel conductance varies from about 150 to 350 pS, while the calcium sensitivity of the maxi-K channel spans 3 orders of magnitude (Latorre et al., 1989; McManus, 1991). Some of these differences have been attributed to experimental conditions, while others may be due to inherent differences in the protein structure. Analysis of genes encoding maxi-K channels from mammalian neural tissue has revealed numerous alternatively spliced variants (Butler et al., 1993; Dworetzky et al., 1994; Pallanck & Ganetzky, 1994; Tseng-Crank et al., 1994), which may explain some of the observed functional differences. This tissue-specific diversity may underlie the various physiological roles of the maxi-K channel. To provide a foundation for understanding the sources of tissue-specific diversity, we have presented a detailed investigation into the biochemical, biophysical, and pharmacological properties of the maxi-K channel purified from bovine aortic smooth muscle.

The Purified ChTX Receptor Consists of an α Subunit and a β Subunit. Identifying the protein composition of the maxi-K channel is an important step toward understanding the molecular basis for the tissue-specific diversity of this channel. The purified ChTX receptor migrated as a large particle, 22 S, on a sucrose density gradient. Analysis of the purified receptor by SDS−PAGE revealed two subunits, α and β, which migrate with apparent molecular weights of 65 and 31 kDa. The β-subunit is heavily glycosylated and is the acceptor for cross-linking with ^{125}I-ChTX. This result is not surprising since the ChTX receptor purified from bovine tracheal smooth muscle similarly consists of two subunits of 62 and 31 kDa (Garcia-Calvo et al., 1994). The β subunit from bovine tracheal smooth muscle is also glycosylated and is the acceptor for cross-linking with ^{125}I-ChTX (Knaus et al., 1994a).

Biochemical and functional data suggest that the β subunit is an integral part of smooth muscle maxi-K channels. Under denaturing conditions, a 31 kDa protein as well as ^{125}I-ChTX cross-linked to the β subunit were specifically immunoprecipitated with antibodies raised against the β subunit (Knaus et al., 1994c). Under nondenaturing conditions, antibodies to the β subunit immunoprecipitated a complex consisting

of α and β subunits (Knaus et al., 1994c). In addition, coexpression of the cloned smooth muscle β subunit (Knaus et al., 1994b) modifies the grating and pharmacology of an *mslo* α subunit expressed in *Xenopus* oocytes (McManus et al., 1995). Thus, the association of the α and β subunits has functional consequences.

Maxi-K channels purified from aortic and tracheal smooth muscle consist of a similar α,β subunit structure. Amino acid sequences obtained from the α subunit of tracheal smooth muscle (Knaus et al., 1994c) were nearly identical with sequences predicted by *mslo*, a gene encoding functional vertebrate maxi-K channels (Butler et al., 1993). Thus, the larger α subunit probably contains the structures that form the ion conduction pathway and that allow for calcium- and voltage-dependent channel gating. The β subunit is closely associated with the α subunit and regulates the gating and pharmacological properties of the α subunit (McManus et al., 1995). In tracheal smooth muscle, the α and β subunits are assembled in approximately a 1:1 stoichiometry (Garcia-Calvo et al., 1994). On the basis of homology with voltage-gated potassium channels (MacKinnon, 1991), we expect that a single smooth muscle maxi-K channel will be formed by a complex of four α and β subunits.

This model raises an issue concerning the size of the α subunit in the purified preparation. The vertebrate *slo* gene encodes a family of alternatively spliced proteins whose size is predicted to be greater than 100 kDa (Butler et al., 1993; Dworetzky et al., 1994; Pallanck & Ganetzky, 1994; Tseng-Crank et al., 1994), while the estimated size of the α subunit in the purified ChTX receptor preparation was about 62 kDa. This discrepancy could result from truncation of the α subunit during processing in the cell or proteolytic degradation during the purification procedure. Recent data suggests that the α subunit is cleaved in the carboxy-terminal half of the molecule by a calcium-dependent process during hydroxylapatite chromatography. The protein fragments cannot be separated upon SDS−PAGE, except under reducing conditions, suggesting the presence of intermolecular disulfide bonds. Antibodies raised against peptide sequences of the α subunit specifically react with a protein of about 125 kDa in Western blots using smooth muscle plasma membranes (Knaus et al., 1995). Thus, the mature α subunit is about 125 kDa and is cleaved during purification. The vast majority of α subunits in the purified preparation appear to have been cleaved. However, the sedimentation coefficient of the ChTX receptor remains unchanged during the whole course of the purification. Furthermore, upon reconstitution into lipid bilayers, the biophysical and pharmacological properties of the purified channel cannot be distinguished from native channels. This suggests that intermolecular forces, including disulfide bonds, are sufficient to maintain the structure of the α subunit after limited proteolytic cleavage. Thus, the purified, reconstituted channel probably exists as a complex of four α and β subunits of 125 and 31 kDa, respectively.

The Purified ChTX Receptor is Sufficient to Reconstitute Fully Functional Maxi-K Channels. When reconstituted into liposomes and incorporated into planar lipid bilayers, the purified ChTX receptor exhibited the biophysical and pharmacological properties expected for a maxi-K channel.

The single-channel conductance values of the purified and native maxi-K channels were identical. Both were 249 pS when the bilayer contained neutral lipids and symmetric 150 mM potassium. The conductance of the purified channel was modified by the lipid composition of the bilayer and the ionic composition of the solutions that bathed the bilayer. For instance, introducing the charged lipid phosphatidylserine into the lipid bilayer increased the conductance value for the purified channel from 249 to 323 pS. This effect of charged lipids has been reported previously for maxi-K channels from skeletal muscle (Moczydlowski et al., 1985). In addition, we found that raising the concentration of potassium caused an increase in the single-channel conductance (Table 1) similar to effects observed with native maxi-K channels (Eisenman et al., 1986; MacKinnon, et al., 1989).

A hallmark of maxi-K channels is that both calcium and voltage regulate gating in a synergistic fashion. Depolarizing the membrane potential is known to increase the fraction of time the maxi-K channel spends in the open or K^+ conductive state (Latorre et al., 1982; Pallotta et al., 1981). The relationship between open probability and voltage for the purified channel was well-described by a Boltzmann function with an e-fold increase in open probability per 11.4 mV. The voltage ($V_{1/2}$), which gave half-maximal activation of the purified channel, shifted to more negative values as the concentration of calcium was increased. The average $V_{1/2}$ value for the purified maxi-K channel was 21 mV when intracellular calcium was 5 μM. The slopes of the voltage-dependent curves were independent of calcium over the examined range of calcium and voltage.

The purified channel was activated by increasing calcium concentrations at a fixed membrane potential. The relationship between calcium and open probability was described by a Hill equation with an average slope of 2.9, indicating that at least three to four calcium ions bind in order to maximally activate the channel. The calcium concentration that causes half-maximal activation ($Ca_{1/2}$) of the purified channel was strongly dependent on membrane potential and decreased as the membrane potential was made more positive. The average $Ca_{1/2}$ for the purified channel was 35 μM when the membrane potential was −20 mV. These measures of the calcium- and voltage-dependent channel gating are within the range of values reported for maxi-K channels from smooth muscle (Latorre et al., 1989; McManus, 1991).

The peptide toxins ChTX and IbTX blocked current through the purified ChTX receptor with nanomolar affinity, and extracellular TEA blocked current through the purified channel with micromolar affinity. The kinetics of toxin block provided a stringent test for the molecular identity of the maxi-K channel. IbTX block of the purified channel was characterized by blocked durations that averaged 10 min. In contrast, shorter blocked durations were observed with ChTX and allowed a more detailed characterization of its interaction with the purified channel. ChTX block of the purified maxi-K channel was consistent with a bimolecular mechanism. Under conditions of physiological ionic strength, the average time for ChTX block of the purified channel was 29 s and the bimolecular association rate constant was 7×10^6 M^{-1} s^{-1}. The K_d value calculated from these kinetic constants was 4.9 nM. These values are similar to values that we determined for ChTX block of the native maxi-K channel from bovine aortic smooth muscle except that the residence time for ChTX on the purified channel is about half of that observed for native channels.

The reconstituted, purified ChTX receptor was incorporated into planar lipid bilayers 34 times from three different preparations; other channel types were not observed. However, two of the 34 purified maxi-K channels that we observed exhibited single-channel conductance values that were approximately one-half of the value expected for the experimental conditions. These two measurements were not included in Figure 4 or in Table 1. Approximately 5% of the time we have observed native maxi-K channels with similar intermediate single-channel conductance values (unpublished observation). In addition, we once observed a purified maxi-K channel that gated between two discrete conductance states, ~165 and ~250 pS. When 10 nM ChTX was added to the extracellular side, both conductance states were blocked. The two conductance states appeared to be derived from a single purified maxi-K channel. We have no concrete explanation for these rare observations. It is possible that these intermediate-conductance maxi-K channels represent a small subpopulation of maxi-K channels with distinct differences in their amino acid sequence, or they may represent channels that have been physically altered in some way. Nevertheless, the smaller conductance maxi-K channels were present in similar proportions in native and purified preparations.

We have shown that the functional properties of the purified ChTX receptor from bovine aortic smooth muscle are nearly identical to those of the native maxi-K channel. Thus, the functional properties of the maxi-K channel are derived from two subunits, α and β, which form the ChTX receptor.

Gating of Purified Channels. Calcium and voltage alter the open probability of the purified channel primarily by modifying the closed durations associated with channel gating. In one instance, we found that a 3-fold increase in intracellular calcium caused a 20-fold decrease in the mean closed durations. In contrast, less than a 2-fold change was observed for the mean open durations. Similarly, we found that membrane potential primarily altered the closed times associated with gating of the purified channel. The mean closed durations decreased exponentially as the membrane potential was increased. The slope of the exponential decline averaged from several experiments was e-fold/12.8 mV. In contrast, the mean open durations increased only slightly with membrane potential. The slope of the exponential increase for mean open times was e-fold/321 mV. Thus, at our level of temporal resolution, the voltage- and calcium-dependent transitions that control gating of the purified maxi-K channel occur primarily between closed states.

Similar to native maxi-K channels (McManus & Magleby, 1991; Moczydlowski & Latorre, 1983), we observed significant variation in calcium sensitivity for different purified channels from the same preparation. For instance, under identical experimental conditions the $Ca_{1/2}$ values for the purified channel ranged over 10-fold while the Hill slopes ranged from 1.3 to 4.3. In addition, $V_{1/2}$ values, which indirectly reflect calcium sensitivity, varied over 54 mV. A number of factors may account for this variation. Some of the variability may be due to expression of more than one splice variant of the channel in this tissue. The vertebrate *slo* gene, which encodes the α subunit, contains four or more splice sites, and individual splice variants can differ in their calcium sensitivity (Tseng-Crank et al., 1994). Evidence for the existence of tissue-expressed splice variants has been recently obtained for the bovine tracheal maxi-K channel (unpublished observations). An additional source of variation may result from physical changes that occur in the channel over time. For instance, we have occassionally observed that over a period of many hours, native and purified maxi-K channels can become less sensitive to calcium. In addition to an irreversible loss in calcium sensitivity, native single maxi-K channels have been observed to undergo discrete, reversible shifts in their open probability (McManus & Magelby, 1988; Moczydlowski & Latorre, 1983). We have found that the purified maxi-K channel also undergoes discrete reversible shifts in gating (Figure 7). Thus, the mode-shifting observed for the maxi-K channel is not derived from regulatory proteins but is an intrinsic channel property. Some of the variation for the purified channel may result from maxi-K channels that we observed gating in different modes but which did not fluctuate between these modes during the course of our experiments.

Variation in calcium sensitivity may also result specifically from interactions between the α and β subunits of the maxi-K channel. It has previously been demonstrated that the expression of the α subunit cloned from mouse brain is sufficient to reconstitute functional maxi-K channels (Butler et al., 1993). However, the calcium sensitivity of the expressed α subunit appeared to be reduced compared to native channels. When α and β subunits were coexpressed, the calcium sensitivity of the expressed heteromeric channels was increased 10-fold relative to the expression of an α subunit alone (McManus et al., 1995). Thus, the interaction of α and β subunits provides a means of regulating calcium sensitivity of the maxi-K channel. Work with the purified ChTX receptor from tracheal smooth muscle suggests that the α and β subunits are present in a 1:1 stoichiometry. However, it is possible that this ratio was not maintained for 100% of the purified maxi-K channels that were incorporated into the lipid bilayer or that coupling between the subunits was disrupted for some channels during purification. Thus, the variation in calcium sensitivity observed for the purified maxi-K channel could also arise from variations in the α and β subunit stoichiometry or from variations in their interactions.

Summary. A simple picture of the molecular components of the maxi-K channel in smooth muscle is emerging. The channel is composed of two distinct subunits, α and β. A multimeric complex of α subunits forms the central ion-conducting pore and contains the components required for voltage- and calcium-dependent channel opening. The β subunit is a closely associated regulatory subunit. These two subunits are sufficient to reconstitute the primary functional properties of the maxi-K channel. It is not yet known whether this structural design is repeated for maxi-K channels from other tissues.

ACKNOWLEDGMENT

We thank Dr. Gregory J. Kaczorowski for discussions and continuous support during the course of this work.

REFERENCES

Adelman, J. P., Shen, K.-Z., Kavanaugh, M. P., Warren, R. A., Wu, Y.-N., Lagrutta, A., Bond, C. T., & North, R. A. (1992) *Neuron 9*, 209−216.

Anderson, C. S., MacKinnon, R., Smith, C., & Miller, C. (1988) *J. Gen. Physiol. 91*, 317−333.

Atkinson, N. S., Robertson, G. A., & Ganetzky, B. (1991) *Science 253*, 551−553.
Banks, B. E. C., Brown, C., Burgess, G. M., Burnstock, G., Claret, M., Cocks, T. M., & Jenkinson, D. H. (1979) *Nature 282*, 415−417.
Barrett, J. N., Magleby, K. L., & Pallota, B. S. (1982) *J. Physiol. 331*, 211−230.
Blatz, A. L., & Magleby, K. L. (1984) *J. Gen. Physiol. 84*, 1−23.
Bradford, M. M. (1976) *Anal. Biochem. 72*, 248−254.
Brayden, J. E., & Nelson, M. T. (1992) *Science 256*, 532−535.
Butler, A., Tsunoda, S., McCobb, D. P., Wei, A., & Salkoff, L. (1993) *Science 261*, 221−224.
Dworetzky, S. I., Trojnacki, J. T., & Gribkoff, V. K. (1994) *Mol. Brain Res. 27*, 189−193.
Eisenman, G., Latorre, R., & Miller, C. (1986) *Biophys. J. 50*, 1025−1034.
Galvez, A., Gimenez-Gallego, G., Reuben, J. P., Roy-Contancin, L., Feigenbaum, P., Kaczorowski, G. J., & Garcia, M. L. (1990) *J. Biol. Chem. 265*, 11083−11090.
Garcia-Calvo, M., Vazquez, J., Smith, M., Kaczorowski, G. J., & Garcia, M. L. (1991) *Biochemistry 30*, 11157−11164.
Garcia-Calvo, M., Knaus, H.-G., McManus, O. B., Giangiacomo, K. M., Kaczorowski, G. J., & Garcia, M. L. (1994) *J. Biol. Chem. 269*, 676−682.
Giangiacomo, K. M., Garcia, M. L., & McManus, O. B. (1992) *Biochemistry 31*, 6719−6727.
Giangiacomo, K. M., Sugg, E., Garcia-Calvo, M., Leonard, R. J., McManus, O. B., Kaczorowski, G. J., & Garcia, M. L. (1993) *Biochemistry 32*, 2363−2370.
Gimenez-Gallego, G., Navia, M. A., Reuben, J. P., Katz, G. M., Kaczorowski, G. J., & Garcia, M. L. (1988) *Proc. Natl. Acad. Sci. U.S.A. 85*, 3329−3333.
Jan, L. Y., & Jan, Y. N. (1992) *Cell 69*, 715−718.
Jones, T. R., Charette, L., Garcia, M. L., & Kaczorowski, G. J. (1990) *J. Pharmacol. Exp. Ther. 255*, 607−706.
Jones, T. R., Charette, L., Garcia, M. L., & Kaczorowski, G. J. (1993) *J. Appl. Physiol. 74*, 1879−1884.
Knaus, H.-G., Eberhart, A., Kaczorowski, G. J., & Garcia, M. L. (1994a) *J. Biol. Chem. 269*, 23336−23341.
Knaus, H.-G., Folander, K., Garcia-Calvo, M., Garcia, M. L., Kaczorowski, G. J., Smith, M., & Swanson, R. (1994b) *J. Biol. Chem. 269*, 17274−17278.
Knaus, H.-G., Garcia-Calvo, M., Kaczorowski, G. J., & Garcia, M. L. (1994c) *J. Biol. Chem. 269*, 3921−3924.
Knaus, H.-G., Eberhart, A., Munujos, P., Kaczorowski, G. J., Schmalhofer, W. A., Warmke, J. W., & Garcia, M. L. (1995) *Biophys. J. 68*, A267.
Latorre, R., & Miller, C. (1983) *J. Membr. Biol. 71*, 11−30.
Latorre, R., Vergara, C., & Hidalgo, C. (1982) *Proc. Natl. Acad. Sci. U.S.A. 79*, 805−809.
Latorre, R., Oberhauser, A., Labarca, P., & Alvarez, O. (1989) *Annu. Rev. Physiol. 51*, 385−399.
Maas, A. J. J., & Den Hertog, A. (1979) *Eur. J. Pharmacol. 58*, 151−156.
MacKinnon, R. (1991) *Nature 350*, 232−235.
MacKinnon, R., & Miller, C. (1988) *J. Gen. Physiol. 91*, 335−349.
MacKinnon, R., Latorre, R., & Miller, C. (1989) *Biochemistry 28*, 8092−8099.
Maruyama, Y., Gallacher, D. V., & Petersen, O. H. (1983a) *Nature 302*, 827−829.
Maruyama, Y., Petersen, O. H., Flanagan, P., & Pearson, G. T. (1983b) *Nature 305*, 228−232.
McManus, O. B. (1991) *J. Bioenerg. Biomembr. 23*, 537−560.
McManus, O. B., & Magelby, K. L. (1988) *J. Physiol. 402*, 79−102.
McManus, O. B., & Magleby, K. L. (1991) *J. Physiol. 443*, 739−777.
McManus, O. B., Helms, L. M. H., Pallanck, L., Ganetzky, B., Swanson, R., & Leonard, R. J. (1995) *Neuron 14*, 645−650.
Moczydlowski, E., Alvarez, O., Vergara, C., & Latorre, R. (1985) *J. Membr. Biol. 83*, 273−282.
Moczydlowski, E., & Latorre, R. (1983) *J. Gen. Physiol. 82*, 511−542.
Pallanck, L., & Ganetzky, B. (1994) *Hum. Mol. Genet. 3*, 1239−1243.
Pallotta, B. S., Magleby, K. L., & Barrett, J. N. (1981) *Nature 293*, 471−474.
Petersen, O. H., & Maruyama, Y. (1984) *Nature 307*, 693−696.
Reinhart, P. H., Chung, S., & Levitan, I. B. (1989) *Neuron 2*, 1031−1041.
Solaro, C. R., & Lingle, C. J. (1992) *Science 257*, 1694−1698.
Stoschek, C. M. (1987) *Anal. Biochem. 160*, 301−305.
Tseng-Crank, J., Foster, C. D., Krause, J. D., Mertz, R., Godinot, N., DiChiara, T. J., & Reinhart, P. H. (1994) *Neuron 13*, 1315−1330.
Vazquez, J., Feigenbaum, P., Katz, G., King, V. F., Reuben, J. P., Roy-Contancin, L., Slaughter, R. S., Kaczorowski, G., & Garcia, M. L. (1989) *J. Biol. Chem. 264*, 20902−20909.
Vergara, C., Moczydlowski, E., & Latorre, R. (1984) *Biophys. J. 45*, 73−76.
Villarroel, A., Alvarez, O., Oberhauser, A., & Latorre, R. (1988) *J. Physiol. (London) 413*, 118−126.
Yellen, G. (1984) *J. Gen. Physiol. 84*, 157−186.

BI951731S